Pergamon

Int. J. Heat Mass Transfer. Vol. 39, No. 6, pp. 1203–1211, 1996

0017–9310/96 \$15.00+0.00

0017–9310(95)00215–4

Transient conjugated mixed convection inside ducts with convection from the ambient

KUAN-TZONG LEE

Department of Mechanical Engineering, Oriental Institute of Technology, Pan-Chiao, Taipei, Taiwan 22064, Republic of China

and

WEI-MON YAN

Department of Mechanical Engineering, Hua Fan College of Humanities and Technology, Shih-Ting, Taipei, Taiwan 22305, Republic of China

(*Received* 26 *October* 1994 *and in final form* 1 *June* 1995)

Abstract—Transient mixed convection heat transfer in both parallel-plate channels and circular pipes subjected to external convection was investigated numerically. The solution takes both wall conduction and wall heat capacity effects into consideration. The governing parameters identified in this work are the outside Nusselt number S, the ratio of Grashof number to Reynolds number Gr/Re, the wall-to-fluid conductivity ratio K, the wall-to-fluid diffusivity ratio A, the dimensionless wall thickness Δ and the Prandtl number Pr. The influences of S, Gr/Re, K, A and Δ on the unsteady characteristics of heat transfer and flow are examined in detail. Predicted results show that wall effects play an important role in unsteady heat transfer. Additionally, it is found that an increase in the outside heat transfer coefficient results in a higher heat transfer exchange and shorter time period required for the system achieving the steady-state condition.

INTRODUCTION

Knowledge of transient mixed convection heat transfer is of importance in a number of different situations such as the starting, ending and change in power level transients, electronic cooling in electronic equipment, cooling and distillation system in chemical processes and ventilation systems.

The studies of combined forced and free convection in vertical parallel plates or pipe have been performed by numerous researchers. Yao [1] presented an analytical solution of developing flow region in a channel with uniform wall temperature or uniform wall heat flux. Quintiere and Muller [2] obtained an approximate solution for mixed convection flow between symmetrically heated vertical parallel plates. The characteristics of mixed convection between asymmetrically heated vertical parallel plates were addressed in refs. [3–6]. Their results showed that the distortion of velocity profile is more severe under asymmetrically heated condition, and the hydrodynamic entry length initially increases rapidly with Gr/Re and then approaches an asymptotic value at large Gr/Re. But the buoyancy effect diminishes the thermal development distance. A critical value of Gr/Re for flow reversal was also provided by Aung and Worku [3]. Aung and Worku [4, 5] concluded that the influence of the thermal buoyancy on the hydrodynamic and thermal characteristics is more pronounced for the case of UWT. Habchi and Acharya [6] indicated that local Nusselt number increases with increasing value of Gr/Re^2. Cheng *et al.* [7] and Lavine [8] presented the closed form solution for laminar fully-developed flow between parallel plates. Ingham *et al.* [9, 10] developed a numerical method to treat the flow reversal in buoyancy aiding and opposing flows. They noted that poor heat transfer results for flow retarded by an opposing buoyancy, but for a large and negative Gr/Re, heat transfer is rather effective. Mixed convection between vertical parallel plates with and without flow reversal was examined by Jeng *et al.* [11] over the range of $Re = 1$–1000. Their results showed that the marching technique using the boundary-layer equations can accurately predicted the heat transfer along the heated wall for $Re \geqslant 50$. Recently, Lin *et al.* [12] numerically studied the mixed convection flow and heat transfer processes in a heated vertical channel. Their results showed that as Gr/Re^2 is relatively large, the flow would become unstable. Similar studies were also performed by refs. [13–17] for pipe flows. Lawrence and Chato [13] numerically investigated the developing flow in a vertical tube with either uniform wall heat flux or uniform wall temperature. Marner and McMillan [14] obtained a numerical solution for fully-developed upflow. A critical range of Gr/Re of flow reversal for developing or developed flow in a pipe subjected to uniform wall temperature was predicted by Zeldin and Schmidt [15]. Tanada *et al.* [16] presented the regime map for laminar and turbulent flow in a uniformly heated vertical pipe. Morton *et al.*

NOMENCLATURE

A	wall-to-fluid thermal diffusivity ratio, α_w/α_f
a, c_1, c_2	constants appearing in equation (5)
b	inside radius of circular pipe or half channel width between parallel plates
Gr	Grashof number, equation (5)
g	gravitational acceleration [m s^{-2}]
h_o	heat transfer coefficient outside the duct [W m^{-2}K^{-1}]
k_f	thermal conductivity of fluid [W m^{-1}K^{-1}]
k_w	thermal conductivity of wall [W m^{-1}K^{-1}]
K	wall-to-fluid thermal conductivity ratio, k_w/k_f
Nu	local Nusselt number based on $T_o - T_e$, equation (11)
Nu_b	local Nusselt number based on $T_{wi} - T_b$, equation (12)
p_m	dynamic pressure [kPa]
P	dimensionless pressure defect, $p_m/(\rho\bar{u}^2)$
Pr	Prandtl number, ν_f/α_f
Re	Reynolds number, equation (5)
r	radial or transverse coordinate
S	outside Nusselt number, $h_0 b/k_w$
t	time [s]
T	temperature [K]
T_a	ambient temperature [K]
T_e	initial or inlet temperature [K]
T_o	outside temperature [K]
u	axial velocity [m s^{-1}]
$\bar{u}$	mean velocity [m s^{-1}]
U	dimensionless axial velocity, $u/\bar{u}$
v	radial or transverse velocity [m s^{-1}]
V	dimensionless radial or transverse velocity, equation (5)
x	axial or longitudinal coordinate [m]
X	dimensionless axial or longitudinal coordinate, equation (5).

Greek symbols

α_f	thermal diffusivity of fluid [m^2 s^{-1}]
α_w	thermal diffusivity of wall [m^2 s^{-1}]
β	thermal expansion coefficient of fluid [1/K]
Δ	dimensionless thickness of duct wall, δ/b
δ	thickness of duct wall [m]
θ	dimensionless temperature, $(T-T_e)/(T_o-T_e)$
θ_b	dimensionless bulk fluid temperature, $\int_0^1 U\theta\eta^a\,d\eta/\int_0^1 U\eta^a\,d\eta$
θ_f	dimensionless fluid temperature
θ_w	dimensionless wall temperature
θ_{wi}	dimensionless interfacial temperature
ν_f	kinematic viscosity of fluid [m^2 s^{-1}]
η	dimensionless radial or transverse coordinate, r/b
ρ	fluid density [kg m^{-3}]
τ	dimensionless time, $t\alpha_f/b^2$.

Superscripts

m	value of mth time step
n	value of nth iteration.

Subscripts

a	at ambient condition
b	bulk fluid quantity
e	at inlet or initial condition
f	of fluid
o	at outside condition
w	of wall.

[17] presented the numerical and experimental results for recirculating flow in aiding and opposing flows.

The effects of wall conduction on the characteristics of purely free convection or mixed convection channel flows have received little attention, especially for transient mixed convection channel flows. Burch *et al.* [18] performed a pioneering study of wall conduction effect on steady natural convection between vertical parallel plates. Similar studies were also performed by Kim *et al.* [19] and Anand *et al.* [20]. Their results showed that the influences of wall conduction on the heat transfer and flow behaviors are significant, particularly for the system with higher Grashof number, larger wall-to-fluid conductivity ratio or thicker wall thickness. As far as steady mixed convection is concerned, Heggs *et al.* [21] studied the influence of wall heat conduction on the steady, recirculating mixed convection flow in a vertical tube. Recently, the unsteady mixed convection heat transfer in a vertical channel was presented by Lin *et al.* [22] and Yan [23]. Their results revealed that the wall heat capacity can have a profound influence on the unsteady mixed convection flow and thermal characteristics. The heat conduction in the wall remains untreated in refs. [22, 23], and hence its effect is not known. But in the study of unsteady forced convection channel flow, Sucec [24, 25], Sucec and Sawant [26], Lin and Kuo [27], Lee and Yan [28] and Yan [29] found that both heat conduction in the wall and wall heat capacity play important roles on the transient conjugated heat transfer.

In the present work, a numerical analysis is performed for unsteady mixed convection heat transfer in a parallel-plate channel or a circular pipe experiencing a sudden change in ambient temperature. The reason for considering a step change in ambient temperature instead of a step change in wall temperature or wall heat flux is that it is a more practical physical situation.

ANALYSIS

In this work, both parallel-plate duct and circular pipe with wall thickness δ are considered, as shown schematically in Fig. 1. The first portion of the duct is insulated, allowing flow to develop. Initially, the whole systems, including the flowing fluid, duct wall and ambient, are at the same uniform temperature T_e, and the flow enters the duct at T_e. At $t = 0$, the ambient temperature is suddenly raised to a new level T_o and maintained at this level thereafter; heat exchange between flow and ambient then starts to occur. The outside heat transfer coefficient between the ambient and the duct wall has the value h_o. Attention is focused on the temporal developments of the hydrodynamic and thermal characteristics in the system after the sudden step change in ambient temperature. To simplify the analysis, the following assumptions are made: (a) the Boussinesq approximation is valid, (b) the fluid is Newtonian, and the viscous dissipation effect is negligible, (c) the flow is laminar and boundary-layer flow, (d) high Peclet number is treated here so that the axial conduction in the flow is negligibly small [30].

Based on the previous discussion and the stated assumptions, the problem can be described by the following governing equations:
continuity equation:

$$\frac{\partial(\eta^a U)}{\partial X} + \frac{\partial(\eta^a V)}{\partial \eta} = 0 \tag{1}$$

axial-momentum equation:

$$\frac{1}{Pr}\frac{\partial U}{\partial \tau} + U\frac{\partial U}{\partial X} + V\frac{\partial U}{\partial \eta} = -\frac{\mathrm{d}P}{\mathrm{d}X} + \frac{1}{\eta^a}\frac{\partial}{\partial \eta}\left(\eta^a \frac{\partial U}{\partial \eta}\right) + \frac{c_1 Gr}{Re}\theta_f \tag{2}$$

energy equation of the fluid:

$$\frac{\partial \theta_f}{\partial \tau} + Pr\left(U\frac{\partial \theta_f}{\partial X} + V\frac{\partial \theta_f}{\partial \eta}\right) = \frac{1}{\eta^a}\frac{\partial}{\partial \eta}\left(\eta^a \frac{\partial \theta_f}{\partial \eta}\right) \tag{3}$$

energy equation of the duct wall:

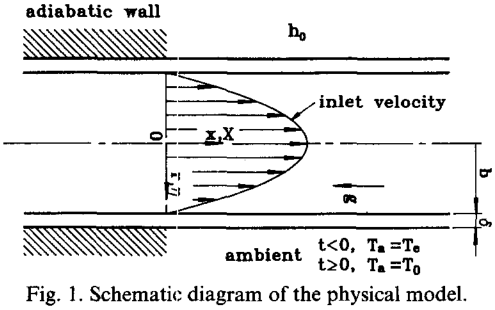

Fig. 1. Schematic diagram of the physical model.

$$\frac{1}{A}\frac{\partial \theta_w}{\partial \tau} = \frac{1}{\eta^a}\frac{\partial}{\partial \eta}\left(\eta^a \frac{\partial \theta_w}{\partial \eta}\right) + \frac{c_2}{Re^2}\frac{\partial^2 \theta_w}{\partial X^2} \tag{4}$$

where the dimensionless quantities are defined as follows:

$$X = c_1 x/(bRe) \quad \eta = r/b \quad U = u/\bar{u}$$

$$V = vRe/(c_1 \bar{u}) \quad P = p_m/(\rho \bar{u}^2) \quad Pr = \nu_f/\alpha_f$$

$$Re = c_1 b\bar{u}/\nu_f \quad K = k_w/k_f \quad A = \alpha_w/\alpha_f$$

$$\Delta = \delta/b \quad \tau = t\alpha_f/b^2 \quad \theta = (T - T_e)/(T_o - T_e)$$

$$Gr = g\beta b^3 (T_o - T_e)/\nu_f^2 \quad S = h_o b/k_w \tag{5}$$

where

$$a = 1 \quad c_1 = 2 \quad c_2 = 4 \quad \text{(for circular pipe)}$$

or

$$a = 0 \quad c_1 = 1 \quad c_2 = 1 \quad \text{(for parallel-plate channel)}.$$

The coefficient, c_2/Re^2, in the energy equation of duct wall is about the order of 10^{-4}–10^{-6}. Hence the axial wall conduction term is small relative to the radial (or transverse) diffusion term and is neglected in the analysis.

The corresponding initial and boundary conditions are:

$$\tau = 0: U = U_{max}(1-\eta^2) \quad \theta_w = \theta_f = 0 \tag{6}$$

$$\tau > 0: X = 0: U = U_{max}(1-\eta^2) \quad \theta_f = 0 \tag{7}$$

$$\eta = 0: \partial U/\partial \eta = \partial \theta_f/\partial \eta = 0 \tag{8}$$

$$\eta = 1: U = 0 \quad \theta_f = \theta_w \quad \partial \theta_f/\partial \eta = K\partial \theta_w/\partial \eta \tag{9}$$

$$\eta = 1+\Delta: \partial \theta_w/\partial \eta - S(1-\theta) = 0 \tag{10}$$

where $U_{max} = 2.0$ (for circular pipe) or $U_{max} = 1.5$ (for parallel-plate channel).

The informative parameter for conjugated heat transfer used to describe the energy transfer into the fluid through the wall–fluid interface is the local Nusselt number base on the temperature difference $T_o - T_e$[22, 23]:

$$Nu = \frac{h \cdot 2b}{k_f} = \frac{q_{wi} \cdot 2b}{(T_o - T_e)k_f} = 2\left.\frac{\partial \theta_f}{\partial \eta}\right|_{\eta=1}. \tag{11}$$

The conventional local Nusselt number based on the temperature difference, $T_{wi} - T_b$, is defined as:

$$Nu_b = \frac{q_{wi} \cdot 2b}{(T_{wi} - T_b)k_f} = \frac{2}{\theta_{wi} - \theta_b}\left.\frac{\partial \theta_f}{\partial \eta}\right|_{\eta=1}. \tag{12}$$

SOLUTION TECHNIQUE

In view of the impossibility to obtain an analytic solution as indicated in the literature survey, the problem defined by the foregoing governing equations was solved by the finite-difference method. The matching conditions imposed at the wall–fluid interface ensure the continuity of heat flux was recast in backward difference for $\partial\theta_f/\partial\eta$ and forward difference for $\partial\theta_w/\partial\eta$. A fully-implicit numerical scheme in which the diffusion and radial (or transverse) convective terms are approximated by central difference, the unsteady term by backward difference and axial advective term by upwind difference is employed to transform the governing equations into finite-difference equations. The finite difference forms of the governing equations are available in the related work [31]. Each system of the finite-difference equations forms a tridiagonal matrix equation which can be efficiently solved by the Thomas algorithm [32].

For given values of Gr/Re, K, A, Δ and S, the solution procedures are described as follows:

(1) At each axial location, guess a dP/dX and solve the axial-momentum equation, equation (2), for U.

(2) Integrate numerically the continuity equation, equation (1), to find V,

$$V = -\frac{1}{\eta^a}\frac{\partial}{\partial X}\int_0^\eta U\eta^a \, d\eta. \tag{13}$$

(3) Solve the energy equations of fluid and wall, equations (3) and (4), simultaneously with the interface matching condition, equation (9).

(4) Check the satisfaction of the conservation of mass and the convergence of U and θ. If yes, a new iteration starts for the next axial location. If not, guess a new dP/dX, and repeat procedures (1)–(4) for the current axial location. The new dP/dX is corrected using the Newton–Raphson method. The iteration procedure is terminated when the following inequalities are satisfied:

$$\left|\int_0^1 U\eta^a \, d\eta - c_3\right| < 10^{-6} \tag{14}$$

$$\frac{\max|\theta_{i,j}^{m,n} - \theta_{i,j}^{m,n-1}|}{\max|\theta_{i,j}^{m,n}|} < 10^{-6} \tag{15}$$

where $c_3 = 0.5$ (for parallel-plate channel) or 1.0 (for circular pipe).

(5) Apply the above procedures from the entrance to downstream region of interest. Repeat procedures (1)–(5) form the start of the transient to the instant at which the steady state is achieved.

It is noted that drastic variations in velocity and temperature are only present in the region closed to the inlet and in the region near the duct wall for the initial period of time. Therefore, nonuniform grids are placed in both axial and radial (or transverse) directions along with the nonuniform time steps. In the radial (or transverse) direction, 81 grid points were deployed where 31 grid points were packed in the wall and 50 in the fluid, while the number of grid points in the axial direction was 101. While the number of grid points are doubled, the deviations in local Nusselt number are less than 1%. Since the size of time increments particularly important at low times, and τ is of order magnitude of the time needed for the inside wall to respond to the sudden change in ambient temperature. A comparison was made for several first time intervals for the case of $Pr = 5.0$, $Gr/Re = 30$, $\Delta = 0.1$ and $S = 10$ in the circular pipe flow. Every subsequent interval is enlarged by 5% over the previous one, i.e. $\Delta\tau_i = 1.05\Delta\tau_{i-1}$. As shown in Table 1, at $\tau = 0.0000903$, the differences in interfacial heat flux for the computation using either 0.000001 or 0.0000001 were within 1%. It is obvious that a first time interval of 0.000001 is sufficiently accurate to describe the flow and heat transfer. All the results presented in this work are computed using the latter one. To check the accuracy of numerical computation, results for steady mixed convection in a vertical tube with zero wall thickness and large $S (S = 100)$ were first obtained. The predicted results compared with those provided by Zeldin and Schmidt [15], the discrepancy was within 2%. Our predictions were also compared with those of Chen *et al.* [33] for the limiting case of purely forced convection ($Gr/Re = 0$) without wall effects. The difference between these two treatments was less than 1%. Through these program tests, the proposed numerical algorithm is considered to be suitable for the present problem.

Table 1. Comparison of the first time interval on the initial transient distributions of Nu at $\tau = 0.0000903$ for the circular pipe flow with $S = 10$

	$\Delta\tau_1 = 0.00001$	$\Delta\tau_1 = 0.000001$	$\Delta\tau_1 = 0.0000001$
$\xi = 0.012697$	5.5446	5.6728	5.6870
$\xi = 0.025906$	5.5446	5.6728	5.6870
$\xi = 0.049986$	5.5446	5.6728	5.6870
$\xi = 0.10243$	5.5446	5.6728	5.6870
$\xi = 0.2$	5.5446	5.6728	5.6870

RESULTS AND DISCUSSION

The forgoing analysis indicates that the heat transfer characteristics in the flow depend on six dimensionless groups, namely, the Prandtl number Pr, ratio of Grashof number to Reynolds number Gr/Re, ratio of wall-to-fluid conductivity K, dimensionless wall thickness Δ, ratio of wall-to-fluid diffusivity A, and outside Nusselt number S.

Figure 2 presents the effects of convective parameter S on the distributions of local Nusselt number Nu based on the temperature difference, $T_0 - T_e$, in vertical pipe and parallel plate channel. During the initial transient period, the local Nu experiences a step increase with time from its initial value of zero to its maximum value and then gradually decreases to the steady-state value. This is due to the predomination of heat conduction in the duct wall, which results in a lower rate of increase in the fluid temperature than in the interface temperature. After the initial transient period, the effects of convection become important for the entrance region, the Nu decreases monotonically with axial distance due to the entrance effect. Beyond this region, the Nu stays constant. This

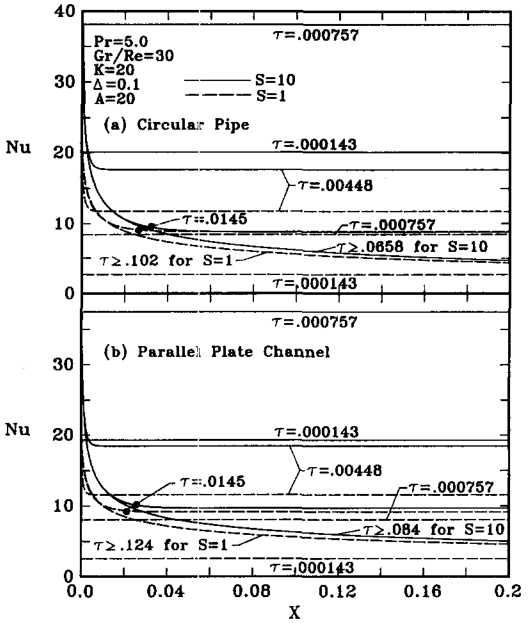

Fig. 2. Effect of S on transient axial distributions of local Nusselt number Nu.

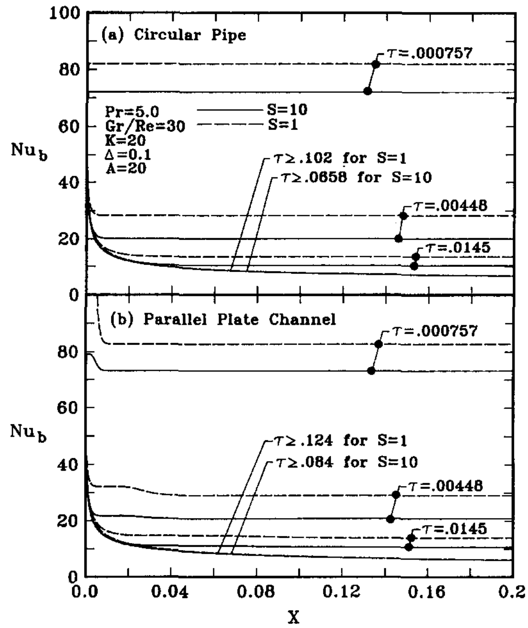

Fig. 3. Effect of S on transient axial distributions of local Nusselt number, Nu_b, based on the temperature difference, $T_{wi}-T_b$.

is due to the fact that the heat transport by convection in the flow does not arrive at this region. Hence, the heat transfer in the flow at this region is still conduction-dominated. Comparison of the results for $S = 10$ and $S = 1$ shows that the heat transfer rate is much more effective for a system with a larger convective parameter $S(= 10)$. This can be solely attributed to the increase in S which can enhance the radial (or transverse) diffusion processes. It is also seen that the larger value of S gives the faster transient because of the decreased thermal resistance between the ambient and the duct wall. A comparison of Figs. 2(a) and (b) shows that the time required for the system to reach the steady-state condition is longer for the case of parallel plate channel. The results of local Nusselt number Nu_b based on the temperature difference, $T_{wi}-T_b$, are also important for the thermal designers. Figure 3 presented the axial distributions of Nusselt number Nu_b. It is observed in Fig. 3 that the Nu_b experiences a step change to a extremely large value at the beginning of transient and then decreases gradually to the steady state value. The discrepancy of Nu_b between the cases of $S = 10$ and $S = 1$ decreases as the time goes. Additionally, the distributions of Nu_b at steady state are indistinguishable for $S = 10$ and $S = 1$.

Shown in Fig. 4 are the distributions of velocity profiles at $X = 0.2$. An overall inspection of Fig. 4 discloses that the velocity profile in the initial transient is parabolic. As the time goes, the profile becomes distorted with the maximum velocity shifting away from the centerline of the duct [in Fig. 4(a)]. This feature is the direct consequence of the fact that the buoyancy force accelerates the fluid near the duct wall, and meanwhile the fluid in the core region decelerates to maintain the overall mass balance. It is worth noting in Fig. 4(a) that the distortion of velocity profile is more significant for the system with a greater $S(= 10)$.

To improve our understanding of heat transfer characteristics in the unsteady mixed convection, Figs. 5 and 6 give the results of the transient distributions local bulk fluid temperatures and interfacial temperatures, respectively. As τ is small, θ_b and θ_{wi} grow very slowly and are uniform in the axial location. The uniformity of θ_b and θ_{wi} is caused by the domination of radial (or transverse) conduction over the axial forced convection during the initial transient. With time elapsing, the effects of both convective heating in the fluid and conduction in the duct wall increase, resulting in considerable increases of θ_b and θ_{wi}. Due to the reason stated previously, an increase S results in a higher θ_b and θ_{wi}. This result is also reflected by the distributions of Nu in Fig. 2.

Figure 7 shows the influences of Gr/Re on the transient distributions of local Nu. At the initial transient stage, the distribution of Nu is uniform and indistinguishable for various values of Gr/Re. This is due to the fact that the heat transfer in the flow is dominated by the conduction at the initial transient stage. After the initial transient period, the effects of convection become important for the region near the entrance. But at downstream region, the distributions of Nu for various values of Gr/Re all approach a asymptotic value. This is simply because the heat transport by convection in the flow does not arrive at this region. Hence the heat conduction still dominates at the region far from the entrance. But as the time proceeds, a larger Nu results for a higher Gr/Re owing to the greater buoyancy effect. It is also noted that for

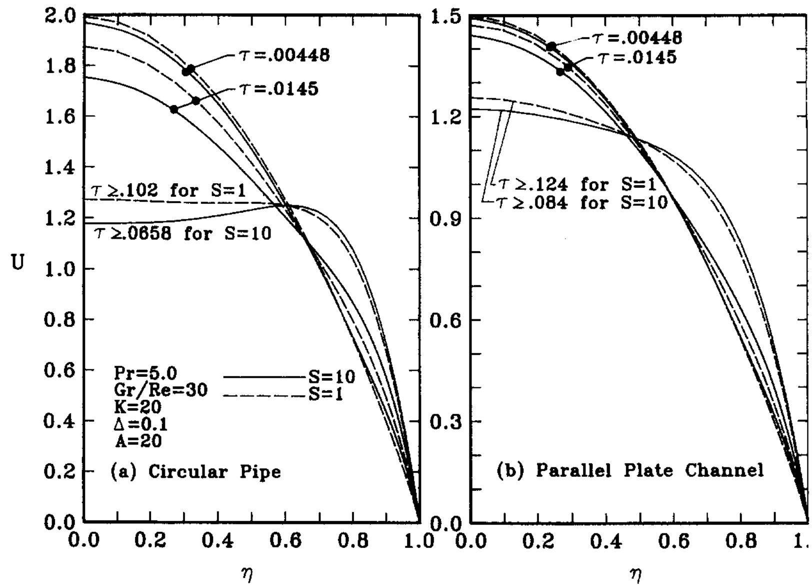

Fig. 4. Effect of S on transient velocity profiles at $X = 0.2$.

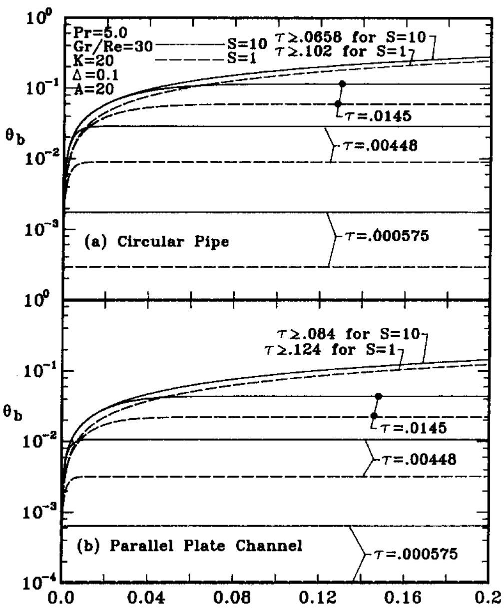

Fig. 5. Effect of S on transient axial distributions of bulk fluid temperature.

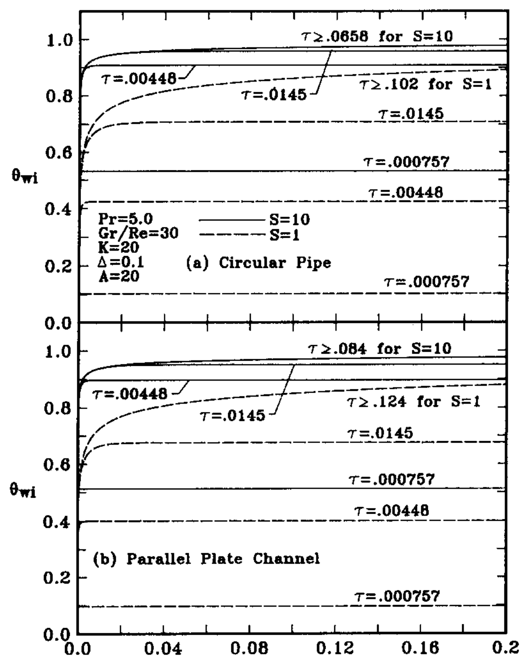

Fig. 6. Effect of S on transient axial distributions of interfacial temperature.

the buoyancy-aiding flow, the time required for the system to reach the steady state is longer for a smaller Gr/Re.

Figure 8 presents the comparison of local Nu between two kinds of duct wall material, namely, stainless steel ($K = 20$, $A = 20$) and carbon steel ($K = 100$ and $A = 100$), which are commonly used in the industrial applications. At the beginning of transient process ($\tau < 0.000506$), a larger Nu is noted for the case of carbon steel. This is made plausible by noting that the predomination of heat conduction in the duct wall is more significant for the system having a greater K. But as the time goes, the trend is reverse and a larger Nu is found for the case of stainless steel. Finally, the steady distributions of Nu for different duct materials exhibit an insignificant discrepancy, and the time required to get to steady state is indistinguishable for the flow through the circular pipe.

Figure 9 presents the comparison of axial distribution of Nu for various wall thickness Δ. At the beginning of the heat transfer process, a slower response in Nu is observed for a system with a thicker

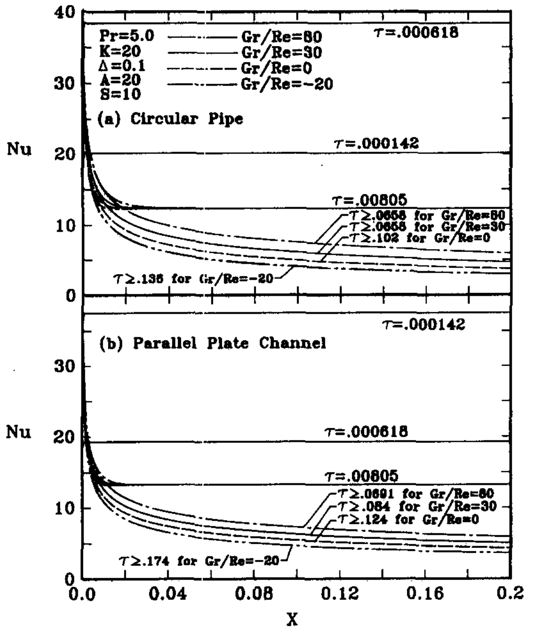

Fig. 7. Effects of Gr/Re on transient axial distributions of local Nusselt number.

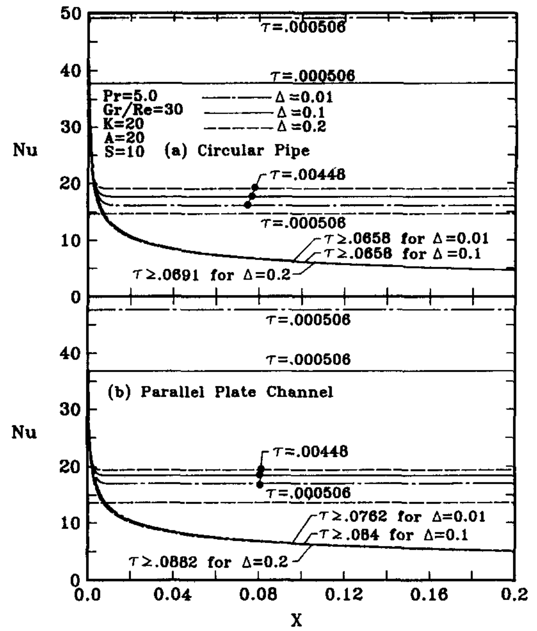

Fig. 9. Effects of Δ on transient axial distributions of local Nusselt number.

wall. This behavior is attributed to the larger heat capacity and wall conduction resistance for the system with a larger Δ. Therefore, the rise of interfacial temperature with time is slower for a thicker wall, which in turn causes a larger Nu. The similar trend was also found by Lee and Yan [28] for the study of purely forced convection. After this early period, the convective effect is dominant for a smaller wall thickness, but heat conduction is still dominant for a thicker wall. Consequently, the distributions of Nu curves are reversed, i.e. Nu is greater for a larger Δ. It is also noted in Fig. 9 that the steady-state distributions of Nu are only slightly influenced by the change of wall thickness.

The effects of the fluid on the local Nusselt number is of practical interest. Figure 10 gives the local Nu for the common heat transfer fluid, air, with $Pr = 0.7$. A comparison of the corresponding curves of Figs. 2 and 10 reveals that a smaller Nu is experienced for a system with air ($Pr = 0.7$) flowing in a pipe, which confirms the general conception that the convective heat transfer is less effective for a system with a lower Pr. In

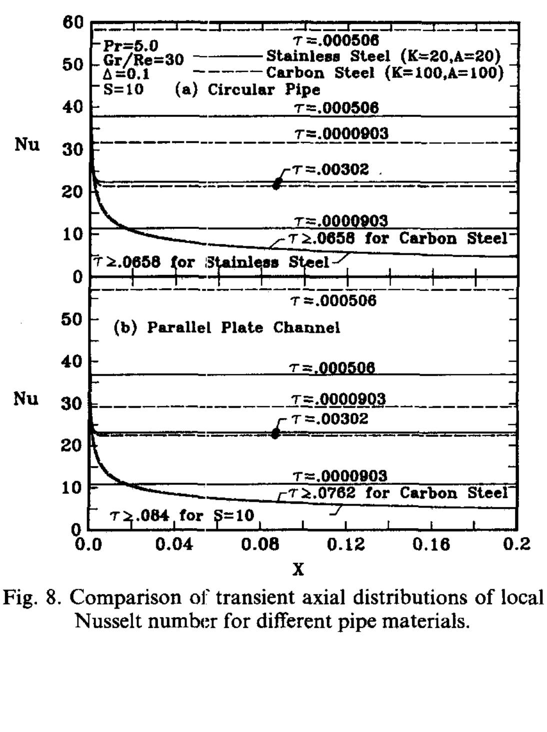

Fig. 8. Comparison of transient axial distributions of local Nusselt number for different pipe materials.

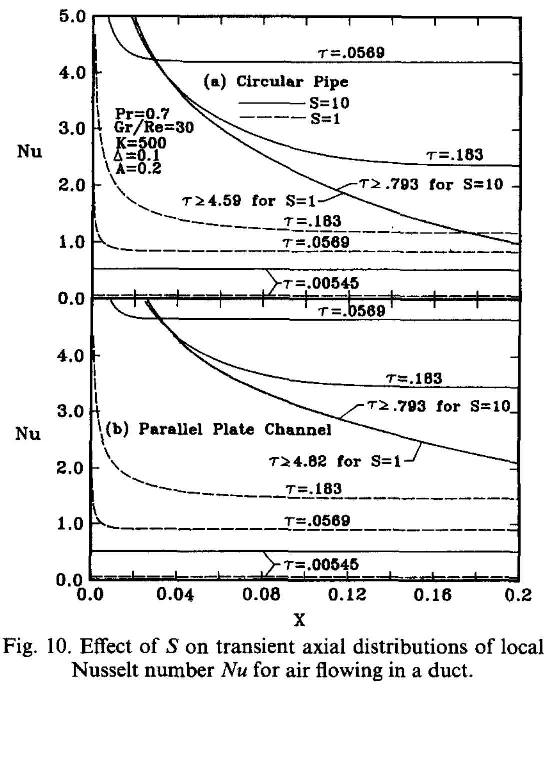

Fig. 10. Effect of S on transient axial distributions of local Nusselt number Nu for air flowing in a duct.

addition, the time required for the flow to reach the steady state is much longer for air flow. Also noted in Fig. 10, for the case of $S = 10$, the Nu shows a step increase with time to its maximum value and then decreases gradually to its eventual steady-state value. On the other hand, the above phenomenon is not found for the case of $S = 1$. Additionally, the axial distributions of Nu at the steady state are indistinguishable by the change of S.

CONCLUSIONS

In the present work, a numerical study has been performed to investigate the unsteady conjugated mixed convection in a circular pipe or parallel-plate channel with convection from ambient. The solutions take wall conduction and wall heat capacity effects into account. What follows is a brief summary of the major results.

(1) The ignorance of the wall effects in the unsteady mixed convection heat transfer would cause a substantial error, especially for the early transient period. Under steady-state conditions, the error in neglecting heat transfer in the duct wall, however, is rather small.

(2) The increase in S results in a greater Nu and shorter time period required for the system achieving the steady-state condition.

(3) The distribution of Nu at steady state is only slightly influenced by the change in Δ or duct material.

(4) The effect of duct material on the time required for the pipe flow to reach the steady-state condition is insignificant, especially for the pipe flow.

Acknowledgement—The financial support of this work by the National Science Council, R.O.C., through the contract NSC82-0401-E211-016 is greatly appreciated.

REFERENCES

1. L. S. Yao, Free and forced convection in the entry region of a heated vertical channel, *Int. J. Heat Mass Transfer* **26,** 65–72 (1983).
2. J. Quintiere and W. K. Muller, An analysis of laminar free and forced convection between finite vertical parallel plates, *J. Heat Transfer* **95,** 53–59 (1973).
3. W. Aung and G. Worku, Developing flow and flow reversal in a vertical channel with asymmetric wall temperature, *J. Heat Transfer* **105,** 299–304 (1986).
4. W. Aung and G. Worku, Mixed convection in ducts with asymmetric wall heat fluxes, *J. Heat Transfer* **109,** 947–951 (1987).
5. W. Aung and G. Worku, Theory of fully developed combined convection including flow reversal, *J. Heat Transfer* **108,** 485–488 (1986).
6. S. Habchi and S. Acharya, Laminar mixed convection in asymmetrically or symmetrically heated vertical channel, *Numer. Heat Transfer* **9,** 605–608 (1986).
7. C. H. Cheng, H. S. Kou and W. H. Huang, Flow reversal and heat transfer of fully developed mixed convection in vertical channel, *J. Thermophys. Heat Transfer* **4,** 375–383 (1990).
8. A. S. Lavine, Analysis of fully developed opposing mixed convection between inclined parallel plates, *Warme- und Stroffubertragung* **88,** 214–222 (1988).
9. D. B. Ingham, D. J. Deen and P. J. Heggs, Two-dimensional combined convection in vertical parallel plate ducts, including situations of flow reversal, *Int. J. Numer. Meth. Engng* **26,** 1645–1664 (1988).
10. D. B. Ingham, D. J. Deen and P. J. Heggs, Flows in vertical channels with asymmetric wall temperatures and including situations where reversal flows occur, *J. Heat Transfer* **110,** 910–917 (1988).
11. Y. N. Jeng, J. L. Chen and W. Aung, On the Reynolds-number independence of mixed convection in a vertical channel subjected to asymmetrical wall temperature with and without flow reversal, *Int. J. Heat Fluid Flow* **13,** 329–339 (1992).
12. T. F. Lin, T. S. Chang and Y. F. Chen, Development of oscillatory asymmetric recirculating flow in transient laminar opposing mixed convection in a symmetrically heated vertical channel, *J. Heat Transfer* **105,** 342–352 (1993).
13. W. T. Lawrence and J. C. Chato, Heat transfer effects on the developing laminar flow inside vertical tube, *J. Heat Transfer* **88,** 241–222 (1966).
14. W. J. Marner and H. K. McMillan, Combined free and forced laminar convection in a vertical tube with constant wall temperature, *J. Heat Transfer* **92,** 559–562 (1970).
15. B. Zeldin and F. W. Schmidt, Developing flow with combined free and forced convection in an isothermal vertical tube, *J. Heat Transfer* **94,** 211–213 (1972).
16. H. Tanaka, S. Maruyama and S. Hatano, Combined forced and natural convection heat transfer for upward flow in a uniformly heated vertical pipe, *Int. J. Heat Mass Transfer* **30,** 165–174 (1987).
17. B. R. Morton, D. B. Ingham, D. J. Keen and P. J. Heggs, Recirculating combined convection in laminar pipe flow, *J. Heat Transfer* **111,** 106–113 (1989).
18. T. Burch, T. Rhodes and S. Acharya, Laminar natural convection between finitely conduction vertical plates, *Int. J. Heat Mass Transfer* **28,** 1173–1186 (1985).
19. S. H. Kim and N. H. Anand and W. Aung, Effect of wall conduction on free convection between asymmetrically heated vertical plates: uniform wall heat flux, *Int. J. Heat Mass Transfer* **33,** 1013–1023 (1990).
20. N. K. Anand and S. H. Kim and W. Aung, Effect of wall conduction on free convection between asymmetrically heated vertical plates: uniform wall temperature, *Int. J. Heat Mass Transfer* **33,** 1025–1028 (1990).
21. P. J. Heggs, D. B. Ingham and D. J. Keen, The effects of heat conduction in the wall on the development of recirculating combined convection flows in vertical tubes, *Int. J. Heat Mass Transfer* **33,** 517–528 (1990).
22. T. F. Lin, C. P. Yin and W. M. Yan, Transient laminar mixed convection heat transfer in vertical flat ducts, *J. Heat Transfer* **113,** 384–390 (1991).
23. W. M. Yan, Transient mixed convection heat transfer in vertical pipe flows, *Int. Commun. Heat Mass Transfer* **19,** 89–101 (1992).
24. J. Sucec, Unsteady conjugated forced convection heat transfer in a duct with convection from the ambient, *Int. J. Heat Mass Transfer* **30,** 1963–1970 (1987).
25. J. Sucec, Exact solution for unsteady conjugated heat transfer in the thermal entrance region of a duct, *J. Heat Transfer* **109,** 295–299 (1987).
26. J. Secec and A. M. Sawant, Unsteady, conjugated, forced convection heat transfer in a parallel plate duct, *Int. J. Heat Mass Transfer* **27,** 95–101 (1984).
27. T. F. Lin and J. C. Kuo, Transient conjugated heat transfer in fully developed laminar pipe flows, *Int. J. Heat Mass Transfer* **31,** 1093–1102 (1988).
28. K. T. Lee and W. M. Yan, Transient conjugated forced convection heat transfer with fully developed laminar flow in pipe, *Numer. Heat Transfer* **23,** 341–359 (1993).
29. W. M. Yan, Transient conjugated heat transfer in channel flows with convection from the ambient, *Int. J. Heat Mass Transfer* **36,** 1295–1301 (1993).

30. R. K. Shah and A. L. London, Laminar flow forced convection in ducts, *Adv. Heat Transfer* [Suppl. 1]. Academic Press, New York (1978).
31. K. T. Lee and W. M. Yan, Numerical study of transient conjugated mixed convection in a vertical pipe, *Numer. Heat Transfer* **26,** 161–179 (1994).
32. S. V. Patanker, *Numerical Heat Transfer and Fluid Flow*, Chaps. 4 and 5. Hemisphere/McGraw-Hill, New York (1980).
33. S. C. Chen, N. K. Anand and D. R. Tree, Analysis of transient laminar convective heat transfer inside a circular duct, *J. Heat Transfer* **105,** 922–924 (1983).